
# Influence of Isotropic and Orthotropic Relationships on the Accuracy of B-spline Based Heterogeneous Graded Finite Element Modeling of Proximal Femur

Uday V. Pise[1], Amba D. Bhatt[2] and R. K. Srivastava[3]

[1]Government Polytechnic Mumbai, India, uvp@mnnit.ac.in
[2]Motilal Nehru National Institute of Technology, India, abhatt@mnnit.ac.in
[3]Motilal Nehru National Institute of Technology, India, rks@mnnit.ac.in

## ABSTRACT

Bone is a highly heterogeneous object. Its composition and structure both vary and depends upon skeletal site, physiological function and age. The goal of this study is to investigate the importance of including material anisotropy in B-Spline based heterogeneous graded (BSBHG) FE model of proximal femur. Five different BSBHG FE models are developed. Out of these five models, four are orthotropic models and one is isotropic model. Each model is simulated in simple stance load condition and their biomechanical response is evaluated and compared with each other as well as those of experimental results given in one of the reference paper for the same specimen in simple stance load condition. The Lagrangian graded element approach is used to assign inhomogeneous isotropic and orthotropic elastic constants in finite element model to improve the performance. Based on the analysis of the two parameters, maximum equivalent Von Mises stress and the displacement in ôzõ direction, comparison is achieved. The displacement and Von Mises results have shown that there is small difference between one of the orthotropic model and the isotropic model while the displacement results of the other two orthotropic models show good agreement with the experimental findings. The global strain prediction accuracy for orthotropic model has improved over isotropic model: the regression coefficient increased from 0.63 to 0.9ð0.96.

**Keywords**: B-Spline, graded element, proximal femur, heterogeneous model, FEA.
**DOI:** 10.3722/cadaps.2012.549-569

## 1 INTRODUCTION

Bone is a complex biological tissue and highly heterogeneous object. Its composition and structure both vary and depend upon skeletal site, physiological function and age. Normally, it consists of compact, dense, and hard (cortical); and spongy (trabeculae with precise pattern) regions. Over the last few years, most of the research has been directed at developing three dimensional finite element (FE) models [2], [11-12], [16-17], [24], [28-29], [31] of bony structures like proximal femur. To generate the three dimensional FE model of any bio-object, CT scan data is one of the primary source of input data. It incorporates information on geometrical topology and bone density distribution based on the relationship between CT numbers and Hounsfield Unit (HU). Furthermore, most of the CT based FE models of bony structures have been used to predict the biomechanical response under static and dynamic load conditions, to calculate the functional adaption of cortical and cancellous bone and to calculate the fracture risk.

In general, behavior of subject specific FE model of bio-objects like proximal femur depends on accurate geometrical topology and method of assignment of material properties. In many prior bone FE studies, [11], [17], [28] material heterogeneity of bone is represented by several sets of elastic moduli, where for each element, modulus is constant within the element, and is computed by power law relation with apparent density. Furthermore, in most of these studies bone mechanical properties are assumed to be isotropic linear elastic. This may be due to limitation in capturing structural anisotropy of trabecular architecture from input CT images [32] and insufficient comprehensive data bank of orthotropic material constants of bone [31]. It was widely recognized that the material constants of bone can be better modeled as orthotropic than isotropic [15], [23].

Also, the works done by Reilly and Burstein [22], Dong and Guo [5] and Iyo et al. [10] indicated that cortical bone is anisotropic or rather transversely isotropic with elastic modulus significantly higher in axial direction ($E_{33}$) than radial ($E_{22}$) and transverse direction ($E_{11}$). Furthermore, the radial and transverse modulus are quiet similar. Doblarè and Garcia [4] and Gómez-Benito et al. [7] have proposed continuum damage and fabric tensor theory to incorporate anisotropy in bone remodeling studies. Similarly, Taylor et al. [31] has used FE modal analysis to determine global orthotropic material constants for whole bone. While Peng et al. [19] have attempted to investigate the effects of orthotropic material property assignment over isotropic model under two load conditions, no attempt has been seen to compare the effects of different orthotropic relations, proposed in literature, to study the biomechanical response of the bone. In our previous study Pise et al. [20], we have presented B-spline based heterogeneous graded (BSBHG) FE model of human proximal femur, where the analysis was carried out with linear isotropic graded element. The model was tested for biomechanical response in simple stance load condition. It was observed that the predicted strain results at different location of the model were in good agreement with the experimental findings of Yosibash et al. [37] except at the neck inferior, for the same specimen. Similarly some discrepancies were also reported for BSBHG FE displacement results with the experimental findings. Therefore, it becomes necessary to study the biomechanical behavior of BSBHG model with assigning of different orthotropic material constants to validate the model fully.

The goal of this study is to investigate the effect of including material anisotropy in B-spline based heterogeneous graded (BSBHG) FE model of human proximal femur. Five BSBHG FE models are developed. Out of these five models one is isotropic and four are orthotropic with different material constant relations as available in literature [14], [19], [31]. Each model is simulated in simple stance load condition and their biomechanical response is evaluated. The evaluated biomechanical response with isotropic and orthotropic material assignments are compared with experimental results given in one of the reference for the same

specimen. The methodology for BSBHG FE model generation along with orthotropic material assignments are given as follows.

## 2 B-SPLINE BASED HETEROGENOUS MODEL FORMULATION

Heterogeneous modeling is the combination of two processes, namely geometric modeling and material modeling. In general, the accuracy of prediction of the mechanical behavior of a heterogeneous bio-object like the femur largely depends upon on accurate representation of its geometry and material. Therefore, B-spline tensor product modeling approach [21] is used here to create a heterogeneous solid model of proximal femur along with graded element [13], [25] to improve the performance of this model. In this modeling strategy, a point ***p****(u, v, w,* ***m****)* in space is represented by four parameters *u, v, w and* ***m*** *: u, v* and *w* representing the parametric space and the vector ***m*** representing the material properties at the point ***p***. The B-spline based hyperpatch model can be as follows:

$$\mathbf{S}(u,v,w) = \sum_{i=0}^{n}\sum_{j=0}^{m}\sum_{k=0}^{l} \mathbf{P}_{i,j,k}\, N_{i,p}(u)\, N_{j,q}(v)\, N_{k,r}(w)\, \mathbf{m}_{i,j,k}$$

where $\mathbf{P}_{i,j,k} = \{\mathbf{P}_{0,0,0}, \mathbf{P}_{0,0,1}, \ldots, \mathbf{P}_{n,m,l}\}$ are control points for the heterogeneous solid volume, Vector **m** represents material distribution (elastic modulus in the present case) within geometric volume, *p, q, r* are the order of the B-spline basis functions $N_{i,p}, N_{j,q}, N_{k,r}$ in the direction of *u, v, w* respectively. The description about the in-house development of this model is available in Bhatt et al. [1] and Warkhedkar et al. [33].

### 2.1 Finite Element (FE) Model formulation

In most of the prior bone FE isotropic and FE orthotropic studies [11], [17], [19], [29], [31], [38], elastic modulus is constant within the element and computed by power law relation with averaged apparent density within the element.

While considering bone as an orthotropic material, Shahar et al. [27] has also demonstrated that local variation (both axial and transverse) direction of elastic modulus and Poisson's ratio in cortical bone is significant. Therefore, in the current study, FE model with orthotropic material assignment has been used with the graded element approach to represent spatial distribution of material property in all directions instead of an average value of elastic modulus for an entire element. Also, due to use of graded element, the problem of assigning material property at the interface element like in cortical-trabeculae interface is eliminated and material heterogeneity can be represented very naturally in all directions. In graded element approach, material property fields like elastic modulus ($E$) and Poisson's ratio ($\nu$) are spatially varying within the element.

The finite element formulation of proximal femur can be governed by the following equation [6].

$$\frac{\partial \sigma_{ij}}{\partial x_j} + b_i = 0 \qquad (1)$$

Here $\sigma_{ij}$ is second order stress tensor and $b_i$ represent body forces (which have been neglected in the analysis). The loading conditions, namely traction forces due to muscles and joint reaction forces on femoral head is given by

$$t_i = \sigma_{ij} n_j \qquad (2)$$

The stress $\sigma$ and strain $\varepsilon$ are related according to

$$\sigma_{ij} = D_{ijkl}\varepsilon_{kl}$$

For heterogeneous materials constitutive matrix $D$ is a function of position which is given as follows

$$D_{ijkl} = \frac{E(x, y, z)}{(1 + \nu)(1 - 2\nu)}\left[\nu\delta_{ij}\delta_{kl} + (1 - 2\nu)\delta_{ik}\delta_{jl}\right]$$

Or

$$E = E(x, y, z) \quad (3)$$

This is further interpolated by element interpolation function to approximate the actual material properties which are written as follows for isotropic and orthotropic material models.

For Isotropic Material:

$$E = \sum_{i=1}^{nne} N_i(x, y, z)E_i = \sum_{i=1}^{nne} N_i E_i$$

For Orthotropic Materials:

$$E_{xx} = \sum_{i=1}^{nne} N_i(x, y, z)E_{xxi} = \sum_{i=1}^{nne} N_i E_{xxi} \qquad E_{yy} = \sum_{i=1}^{nne} N_i(x, y, z)E_{yyi} = \sum_{i=1}^{nne} N_i E_{yyi}$$

$$E_{zz} = \sum_{i=1}^{nne} N_i(x, y, z)E_{zzi} = \sum_{i=1}^{nne} N_i E_{zzi} \qquad E_{xy} = \sum_{i=1}^{nne} N_i(x, y, z)E_{xyi} = \sum_{i=1}^{nne} N_i E_{xyi}$$

$$E_{yz} = \sum_{i=1}^{nne} N_i(x, y, z)E_{yzi} = \sum_{i=1}^{nne} N_i E_{yzi} \qquad E_{zx} = \sum_{i=1}^{nne} N_i(x, y, z)E_{zxi} = \sum_{i=1}^{nne} N_i E_{zxi} \quad (4)$$

Where $nne$ is number of nodes in an element.

## 2.2 Model Generation and Determination of Material Properties

To generate a heterogamous model of a bio-object, CT scan data is used as the primary source of input data. In the present study, geometrical data of proximal femur, material properties of cortical and cancellous bones in the form of CT slices have been downloaded from the URL: www.bgu.ac.it/~zohari/CT_FF.html [37] and initially processing is done with the help of MIMICS (Materialise' interactive medical imaging control system, a medical image processing software package, www.materrialise.com). The data belong to a 30 year-old male with following parameters: 140 kV p, 250 mA s, 0.75 mm slice thickness, axial scan without overlap with pixel size of 0.78 mm. Total CT scan data contains 97 slices, out of these 3 slices have been neglected from distal end. Thereafter, CT images in pixel data form are cropped to limit the point cloud data in order to avoid noise. Noise due to strain gauge wire and bolts is removed from each slice. The cropped slices are organized and segmented between 100 and 2000 Hounsfield Unit (HU) to identify both trabecular and cortical bone. The processed gridded data points of the group of the slices are treated as control points. Further

processing of the data was done with in-house developed modeling software [1]. The B-spline triparametric hyperpatch [1], [33] approach is used to represent solid model of proximal femur. An in-house generalized algorithm based on MATLAB and C platform is used to find out control polyhedron from the control points by applying B-spline hyperpatch approach.

Thus, in the proposed methodology, mesh is generated from the processed points by varying increments in parametric values in the three parametric directions namely u, v and w; and material properties are computed and assigned at each point (nodal point). The developed heterogeneous solid model of proximal femur with graded element is used for FE analysis after the convergence test. To carry out convergence test the twelve BSBHG models have been generated using varying mesh density for single-legged stance loading and boundary conditions [20]. The convergence test result showed that FE results of BSBHG model get optimized between 60,000 to 86,250 degrees of freedom. In the present study, FE model with 66,240 degrees of freedom has been used to achieve reasonable accuracy with reduced computational cost.

### 2.3 Material Properties for Cortical and Cancellous Bone

This section presents a general description of anisotropic and four orthotropic material models used in this study. In general, bone material properties are obtained through apparent density. Two linear relationships between apparent density and HU are used to determine the magnitude of apparent density for cortical and cancellous region of proximal femur. For dense cortical bone, it is assumed that apparent density ($\rho$) is 1.9 g/cm$^3$ [29], [37] associated with maximum HU value 1752 and apparent density of water to be 0 g / cm$^3$ associated with 0 HU.

$$\rho = \frac{1.9 \times h}{1752} \quad (5)$$

For cancellous bone of proximal femur, a linear relationship between HU number and bone apparent density is assumed [23]. Here h represents HU value.

$$\rho = 131 + 1.067h \quad (6)$$

The next stage in the FE model definition process is to calculate the material constants from apparent density. In the present study, the following five relationships have been used to evaluate elastic constants.

A: Isotropic material model

In this material model definition, elastic constants are evaluated by using Wirtz et al. [34] power model as follows.

$$E = \begin{cases} 1094\rho^{2.000} \\ 2065\rho^{2.000} \end{cases} \quad \nu = \begin{cases} 0.3 & 100 \le h \le 349 \\ 0.36 & 350 \le h \le 2000 \end{cases} \quad (7)$$

In above relations, the unit of $E$ (Young's modulus) is MPa and that of $\rho$ (apparent density) is g/cm$^3$. $\nu$ is the Poisson's ratio.

B: Orthotropic model 1: Taylor's material model [31]

In this material model, a quadratic distribution of elastic constants from lowest to highest apparent density values are used for the entire bone (cortical and cancellous bone)

$$E_{11} = E_{11max}\rho^2/\rho^2_{max} \qquad G_{12} = G_{12max}\rho^2/\rho^2_{max} \qquad \nu_{12} = 0.4$$

$$E_{22} = E_{22max}\rho^2/\rho^2_{max} \qquad G_{23} = G_{12max}\rho^2/\rho^2_{max} \qquad \nu_{23} = 0.23$$

$$E_{33} = E_{33max}\rho^2/\rho^2_{max} \qquad G_{13} = G_{12max}\rho^2/\rho^2_{max} \qquad \nu_{13} = 0.25 \qquad (8)$$

where, E (Young's modulus is in MPa, G (shear modulus) in MPa and $\rho$ (apparent density) in kg / m$^3$

$$E_{11max} = 13.4 \text{ Gpa} \qquad G_{12max} = 5710 \text{ Mpa}$$

$$E_{22max} = 14.10 \text{ Gpa} \qquad G_{23max} = 6580 \text{ Mpa}$$

$$E_{33max} = 22.9 \text{ Gpa} \qquad G_{13max} = 7110 \text{ Mpa} \qquad (9)$$

$E_{11max}$, $E_{22max}$ and $E_{33max}$ are taken from predicated Taylor's FE model while $G_{12max}$, $G_{23max}$ and $G_{13max}$ are taken from ultrasound experimental values of dense cortical region [28].

C: Orthotropic model 2: Peng material model [19]

In this material model, both the cortical and cancellous bone is assumed to be transversely isotropic material. Normally it represents same properties in all direction of the transverse plane and significantly different properties in the longitudinal direction. A quadratic distribution of shear modulus from lowest to highest apparent density values are used for the whole bone. In turn, material model definition is as follows.

Cancellous bone

$$E_{11} = 1157\,\rho^{1.78} \text{ Mpa} \qquad G_{12} = G_{12max}\rho^2/\rho^2_{max} \qquad \nu_{12} = 0.4$$

$$E_{22} = 1157\,\rho^{1.78} \text{ Mpa} \qquad G_{23} = G_{12max}\rho^2/\rho^2_{max} \qquad \nu_{23} = 0.25$$

$$E_{33} = 1904\rho^{1.64} \text{ Mpa} \qquad G_{13} = G_{12max}\rho^2/\rho^2_{max} \qquad \nu_{13} = 0.25 \qquad (10)$$

Cortical bone

$$E_{11} = 2314\,\rho^{1.57} \text{ Mpa} \qquad G_{12} = G_{12max}\rho^2/\rho^2_{max} \qquad \nu_{12} = 0.45$$

$$E_{22} = 2314\,\rho^{1.57} \text{ Mpa} \qquad G_{23} = G_{12max}\rho^2/\rho^2_{max} \qquad \nu_{23} = 0.25$$

$$E_{33} = 2065\rho^{3.09} \text{ Mpa} \qquad G_{13} = G_{12max}\rho^2/\rho^2_{max} \qquad \nu_{13} = 0.25$$

where

$G_{12max}$ = 5710 Mpa $\quad G_{23max}$ = 6580 Mpa $\quad G_{13max}$ = 7110 Mpa $\qquad$ (11)

D: Orthotropic model 3: "Peng - Krone" material model

In this material model, we have combined two models: elastic constant $E$ (Young's modulus ) is evaluated from the relationship reported in Peng et al. [19], while for elastic constant $G$ ( shear modulus) a constant magnitude ( independent on apparent density) [14] has been used for both cancellous and cortical bone. The material model definition is written as follows.

Cancellous bone

$E_{11}$=1157 $\rho^{1.78}$ MPa $G_{12}$=370 MPa $\nu_{12}$= 0.3

$E_{22}$=1157 $\rho^{1.78}$ MPa $G_{23}$=399 MPa $\nu_{23}$= 0.3

$E_{33}$=1904$\rho^{1.64}$ MPa $G_{13}$=399 MPa $\nu_{13}$= 0.3 (12)

Cortical bone

$E_{11}$=2314 $\rho^{1.57}$ MPa $G_{12}$=3.60 GPa $\nu_{12}$= 0.45

$E_{22}$=2314 $\rho^{1.57}$ MPa $G_{23}$=3.30 GPa $\nu_{23}$= 0.3

$E_{33}$=2065$\rho^{3.09}$ MPa $G_{13}$=3.30 GPa $\nu_{13}$= 0.3 (13)

E: Orthotropic model 4: "Rho – Peng" material model

This model is created by combining Rho et al. [23] and Peng et al. [19]. A linear relationship from Rho et al. [23] between $E$ (Young's modulus) and $\rho$ (apparent density is used for both cortical and cancellous bone while for $G$ (shear modulus) a quadratic distribution from lowest to highest apparent density values are used for whole bone [19]. The model definition is given as below.

Cancellous bone

$E_{11}$= -657+3.91$\rho$ $G_{12}= G_{12\max}\rho^2/\rho^2_{\max}$ $\nu_{12}$= 0.3

$E_{22}$= -506+3.64$\rho$ $G_{23}= G_{12\max}\rho^2/\rho^2_{\max}$ $\nu_{23}$= 0.3

$E_{32}$= -331+4.56$\rho$ $G_{13}= G_{12\max}\rho^2/\rho^2_{\max}$ $\nu_{13}$= 0.3 (14)

where $\rho$ is kg / m$^3$ and $E_{11}$, $E_{22,}$ *and* $E_{33}$ are in MPa.

Cortical bone

$E_{11}$= -6.087+0.010$\rho$ $G_{12}= G_{12\max}\rho^2/\rho^2_{\max}$ $\nu_{12}$= 0.45

$E_{22}$= -4.007+0.009$\rho$ $G_{23}= G_{12\max}\rho^2/\rho^2_{\max}$ $\nu_{23}$= 0.3

$E_{33}$= -6.142+0.014$\rho$ $G_{13}= G_{12\max}\rho^2/\rho^2_{\max}$ $\nu_{13}$= 0.3 (15)

where $\rho$ is kg / m$^3$ and $E_{11}$, $E_{22,}$ $E_{33}$ are in GPa and $G_{12\max}$= 5710 MPa $G_{23\max}$=6580 MPa $G_{13\max}$= 7110 MPa.

In all above orthotropic models, all parameters are set in Cartesian co-ordinate system of Femur with direction anterior-posterior (11), medial-lateral (22), and superior-inferior (33) (see Fig. 1). Though the empirical equations given by Rho et al. were in cylindrical co-ordinates, this change in co-ordinate system would not invalidate the findings as this study is used for comparing different numerical solutions. The BSBHG model with the three principal directions is shown in Fig.1.

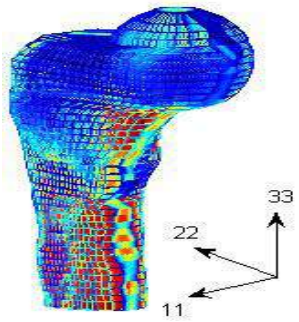


Fig.1: BSBHG model with orthotropic directions.

All the chosen orthotropic E-$\rho_{(app)}$ relations specifies two distinct density region, one for trabecular bone and second for cortical bone. The map of the mechanical properties in all orthotropic relations is shown in Fig. 2-4. A close observation of Fig. 2 indicates that the magnitude of Young's moduli ($E_{11}$, $E_{22}$, and $E_{33}$) are significantly higher for Taylor's and Rho-Peng orthotropic model for all density values varying from lowest to highest. Whereas other two orthotropic relations are same in terms of evaluation of Young's moduli and one shows lower bound for the density values of interest (0.2 to 2.0 g/cm$^3$) derived after the model description.

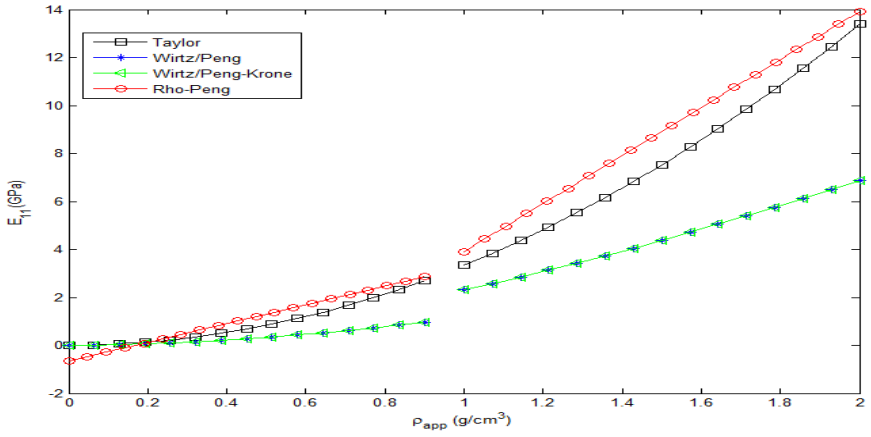


Fig. 2: Relation between Young's modulus ($E_{11}$) and apparent density for the four selected orthotropic density-elasticity relationships for typical human bone.

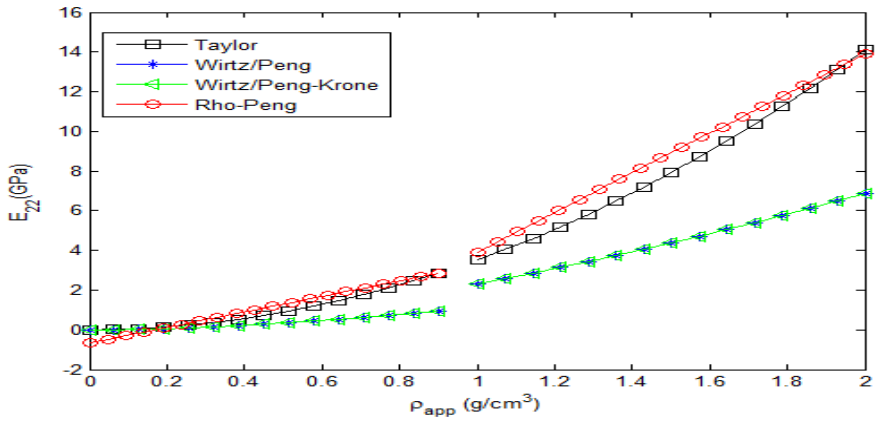


Fig. 3: Relation between Youngôs modulus ($E_{22}$) and apparent density for the four selected orthotropic density-elasticity relationships for typical human bone.

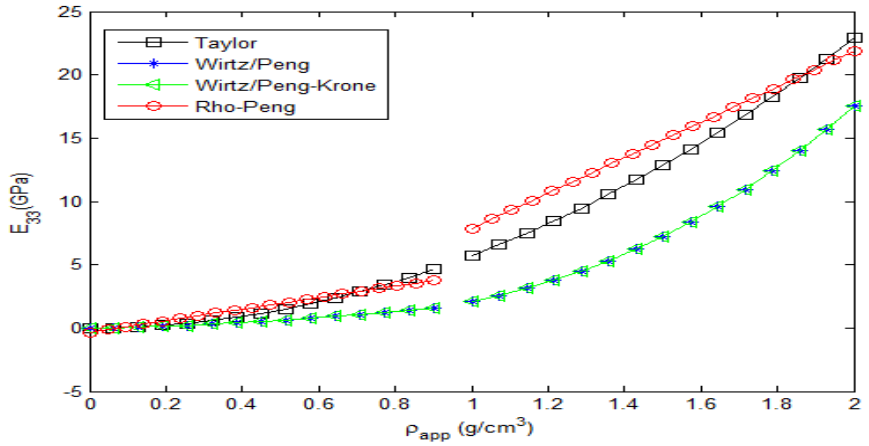


Fig. 4: Relation between Youngôs modulus ($E_{33}$) and apparent density for the four selected orthotropic density-elasticity relationships for typical human bone.

More recently, ôorthotropic ratioô (anisotropic ratio) is used to quantify the degree of anisotropy. Orthotropic ratio is defined as longitudinal Youngôs modulus to other transverse Youngôs modulus (i.e. $E_{33}$ / $E_{11}$ or $E_{33}$ / $E_{22}$). For bony structure orthotropic ratios are location dependent. In literature, it is reported that orthotropic ratios for cortical bone of human femur lies in the range of 1.4 to 2.35 [5] [22], and for cancellous bone it lies between 1 and 4 [31]. In present study, Taylorôs orthotropic model shows same orthotropic ratio ($E_{33}$ / $E_{11}$=1.72, $E_{33}$ / $E_{22}$=1.623) for both cancellous and cortical bone. This is due to the fact that a single relation has been used to define the properties of cortical and cancellous bone. Also this model doesnôt yield location dependent anisotropy ratio. While in other three orthotropic models (Wirtz/Peng model, Wirtz/Peng-Krone model, Rho-Peng model), orthotropic

ratio is location dependent and density dependent. The orthotropic ratios for these models are continuously varying with apparent density in a valid range (Fig. 5).

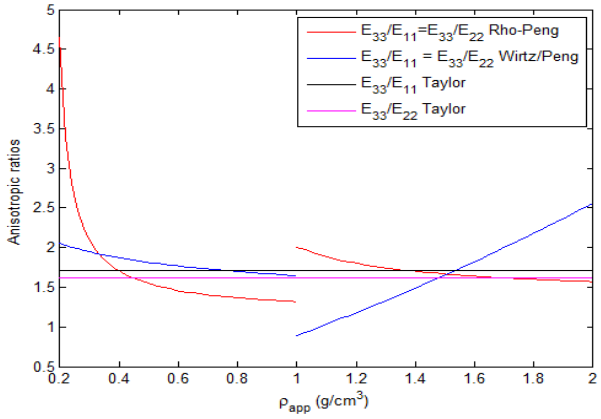


Fig. 5: Relation between orthotropic ratios and apparent density for the four selected orthotropic density-elasticity relationships for typical human bone.

## 3 LOADING CONDITIONS

In this section, numerical experiments are implemented on all material models to testify the performance of BSBHG FE model. The graded FE model (with 66,240 degrees of freedom) is then simulated for simple stance position similar to one given by Yosibash et al. [37]. In which a force of 1500 N was applied on specimen in four-inclination angle i.e. $0^0$, $7^0$, $15^0$ and $20^0$ respectively along femoral shaft axis. A typical loading and boundary condition with $0^0$ is shown in Fig. 6. The displacement result obtained from the above reference is termed as experimental. Similar conditions are simulated theoretically in the present work for all five material models which is theoretical results based on B-spline based heterogeneous graded (BSBHG) modeling.

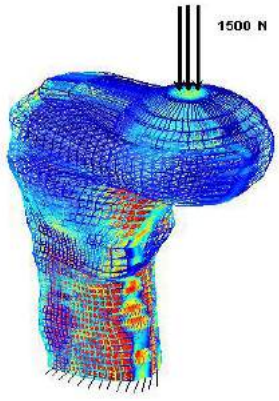


Fig. 6: B-spline based graded FE model, with loading and boundary condition in simple stance configuration.

The displacement result and strain results obtained from four orthotropic material models are compared with isotropic model. All the evaluated results are also compared with experimental results which are given below.

## 4 RESULTS

Two parameters, head displacement in ‘z’ direction ($U_z$) and strain at neck superior ($\epsilon_z$), neck inferior ($\epsilon_z$), shaft medial ($\epsilon_z$), and shaft lateral ($\epsilon_1$) are evaluated from the four BSBHG orthotropic models.

### 4.1 Comparison between Predicted and Experimental Displacement ($U_z$)

The evaluated head displacement in ‘z’ direction ($U_z$) for all orthotropic models and isotropic models along with experimental findings of Yosibash et al. [34], are tabulated for all load configurations in Tab. 1. Further, all the results are compared to establish relationship between all the studies which is shown in Fig. 7.

| Angle (degree) | Isotropic material model ($U_I$) mm | Orthotropic material models | | | | Yosibash's Exp. Results [37] ($U_E$) mm |
|---|---|---|---|---|---|---|
| | | Taylor [31] ($U_{OT}$) mm | Wirtz/Peng ($U_{OWP}$) mm | Wirtz/Peng-Krone ($U_{OWPK}$) mm | Row-Peng ($U_{OR}$) mm | |
| 0º | 0.886 | 0.592 | 0.833 | 0.736 | 0.613 | 0.45 |
| 7º | 0.624 | 0.442 | 0.596 | 0.506 | 0.460 | 0.19 |
| 15º | 0.329 | 0.205 | 0.311 | 0.230 | 0.217 | 0.26 |
| 20º | 0.227 | 0.175 | 0.198 | 0.142 | 0.178 | 0.25 |

Tab. 1: Overall displacement response for all material models and Yosibash's experimental displacement in a simple stance load conditions.

To compare evaluated orthotropic proximal femur head displacements results with evaluated isotropic head displacement results, four non dimensional parameters are defined which may make results more comprehensible. All parameters represent the relative differences between the maximum value of ‘z’ displacement in all load configurations for all orthotropic material models discussed earlier.

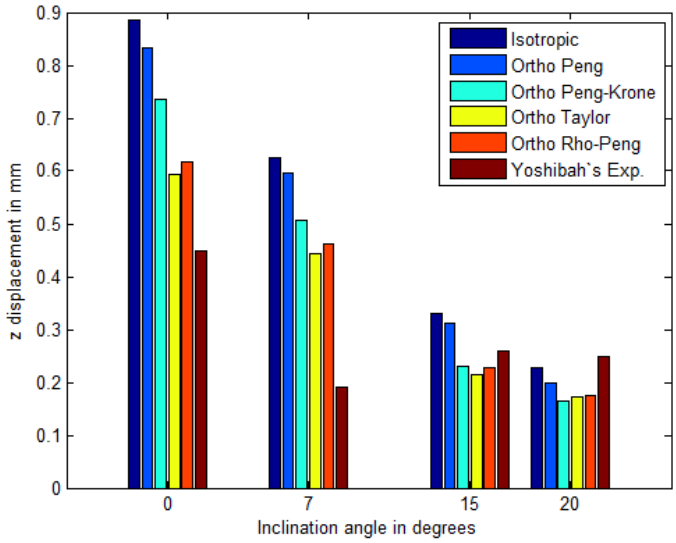


Fig. 7**:** FEA displacement results of BSBHG model using isotropic and orthotropic relations compared to Yosibashís experimental observations for 1500 N axial load.

These four non-dimension parameters are listed as follows.

$$\frac{\square_{\square\square}}{\square_{\square}} = \frac{\square\square_{\square\square} - \square\square_{\square}}{\square_{\square}} \times 100 \qquad \frac{\square_{\square\square\square}}{\square_{\square}} = \frac{\square\square_{\square\square\square} - \square\square_{\square}}{\square_{\square}} \times 100$$

$$\frac{\square_{\square\square\square}}{\square_{\square}} = \frac{(\square_{\square\square\square} - \square\square_{\square})}{\square_{\square}} \times 100 \qquad \frac{\square_{\square\square}}{\square_{\square}} = \frac{(\square_{\square\square} - \square\square_{\square})}{\square_{\square}} \times 100 \qquad (16)$$

where, $U_I$ represent the magnitude of maximum femur head displacement in ôzô direction for isotropic material model while $U_{OT,}$ , $U_{OWP}$ , $U_{OWPK}$, $U_{OR}$ are displacement magnitude of femur head in ôzô direction for Taylor, Wirtz/Peng, Wirtz/Peng-Krone and Rho-Peng orthotropic models respectively. Tabulated results are shown in Tab. 2.

Similarly, to compare evaluated orthotropic and Isotropic head displacements results with experimental results of head displacement, five parameters are defined which are written as follows. Results for these parameters are calculated for all load condition except 7˚ load configuration. This is because the experimental finding for this load configuration is not reliable.

| Loading angle | $U_{OT}/U_I$(%) | $U_{OWP}/U_I$(%) | $U_{OWPK}/U_I$(%) | $U_{OR}/U_I$ (%) |
|---|---|---|---|---|
| 0º | -33.10 | -5.80 | -16.90 | -30.60 |
| 7º | -29.10 | -4.40 | -18.90 | -25.90 |
| 15º | -37.60 | -5.00 | -30.10 | -34.06 |
| 20º | -22.90 | -12.70 | -37.44 | -21.50 |

Tab. 2: Effects of load configurations on parameters $U_{OT}/U_I$, $U_{OWP}/U_I$, $U_{OWPK}/U_I$ and $U_{OR}/U_I$.

$$\frac{\quad}{\quad} = \frac{(\quad)}{\quad} \times 100 \qquad \frac{\quad}{\quad} = \frac{(\quad)}{\quad} \times 100$$

$$\frac{\quad}{\quad} = \frac{\quad}{\quad} \times 100 \qquad \frac{\quad}{\quad} = \frac{\quad}{\quad} \times 100$$

$$\frac{\quad}{\quad} = \frac{\quad}{\quad} \times 100 \qquad (17)$$

where, $U_E$ represent the reported experimental magnitude of maximum femur head displacement in ôzõ direction. Calculated results are shown in Tab. 3.

| Loading angle | $U_I/U_E$ (%) | $U_{OT}/U_E$ (%) | $U_{OWP}/U_E$ (%) | $U_{OWPK}/U_E$ (%) | $U_{OR}/U_E$ (%) |
|---|---|---|---|---|---|
| 0º | 96.80 | 31.70 | 85.33 | 63.60 | 35.50 |
| 15º | 26.50 | 21.15 | 20.00 | -11.53 | -16.15 |
| 20º | -9.20 | 30.00 | -20.80 | -43.20 | -28.80 |

Tab. 3: Effects of load configurations on parameters $U_I/U_E$, $U_{OT}/U_E$, $U_{OWP}/U_E$, $U_{OWPK}/U_E$ and $U_{OR}/U_E$.

It is observed from Tab.2 that the relative difference between the displacement results of Wirtz/Peng orthotropic model and isotropic model is reasonably small for all load conditions while the difference between Taylor model and Row-Peng model with isotropic model is 21.5 to 37% for all load conditions. Furthermore, columns 2 and 5 of Tab. 3 indicates that the difference between the experimental results and those of Taylor material model and Row-Peng material model results are consistent for all load conditions. They are also near to Yosibashís experimental measurements. The displacement results of Wirtz/Peng model shows similar pattern as Taylor and Rho-Peng model for 15˚ and 20˚ load configurations. The results are not similar for 0˚ load configuration. By comparison Wirtz/Peng-Krone and Isotropic models show distinct results for all load configurations in comparison with experimental results.

### 4.2 Comparison of FE Models *vs.* Experimental Strain Findings

A linear least square regression between the experimentally measured strains and predicted strains by each model is performed to quantify prediction accuracy. The goodness of prediction is expressed by the coefficient of linear regression $R^2$, slope and intercept of the curve. These metrics provide a global indication on the goodness of the prediction. And to know local errors from each single prediction one should calculate the local error metrics like or maximum error (peak error) and the average error. Therefore, for isotropic material model and each orthotropic material model simulation, the correlation, slope, intercept, maximum (peak) error and average error (root mean square error i.e. RMSE) and RMSE % are calculated. Usually, RMSE% is calculated by dividing the square root of the mean of the squared errors between numerical and experimental strains (RMSE) by the highest strain value obtained across the specimen. The regression results are indicated in Fig. 8-12.

The strains obtained due to FE analysis (theoretical) for isotropic and all orthotropic models are compared with the Yosibash et al. experimental findings at neck superior ($\epsilon_2$), neck inferior ($\epsilon_2$), shaft medial ($\epsilon_2$), and shaft lateral ($\epsilon_1$) (see Fig. 8-12 and Tab. 4). The predicted (theoretical) strain results for all the four location of the proximal femur correlate very strongly with experimental values for all orthotropic models. The coefficient of linear regression $R^2$ for all orthotropic models are in the range of 0.92 to 0.96. These $R^2$ values are significantly higher than isotropic model regression coefficient $R^2$ = 0.63. For Wirtz/Peng and Wirtz/Peng-Krone model, the regression line slopes are very close to unity. But for Taylorís model and Rho-Pengís model, slope of regression line is slightly low than one, indicating that globally these two models underestimate the strains. This may be due to their upper bound density-modulus relation in both cancellous and cortical region (see Fig. 2-4). The y-intercepts are found between 54.02 and 115.59 for all orthotropic relations. The regression slope and intercept for the isotropic model are 0.600 and 130.28 respectively.

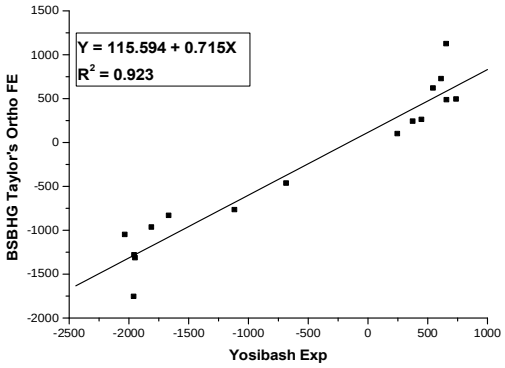


Fig. 8: Linear regression of predicted vs. experimental strain (με) in Taylor orthotropic model [14].

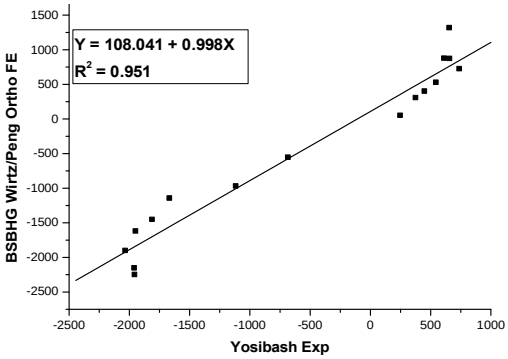


Fig. 9: Linear regression of predicted vs. experimental strain (με) in Wirtz [34] /Peng [19] orthotropic model.

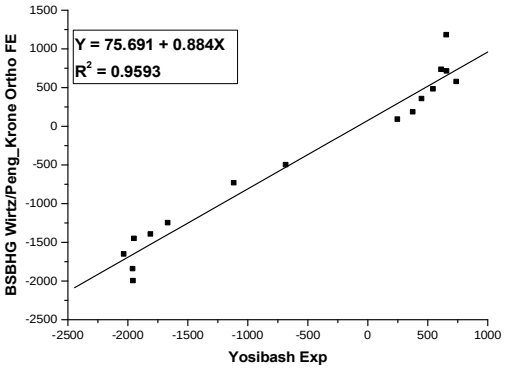


Fig. 10: linear regressions of predicted vs. strain (με) in Wirtz [34] /Peng-Krone orthotropic model.

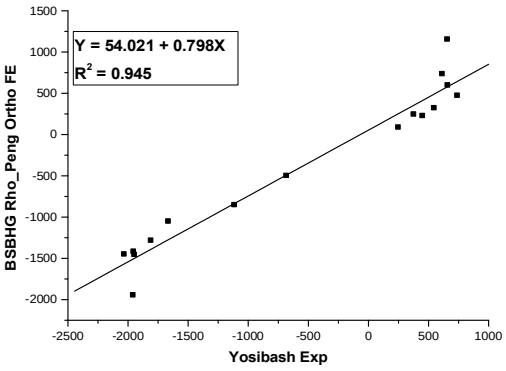


Fig. 11: Linear regression of predicted experimental experimental strain (με) in Rho-Peng Orthotropic model.

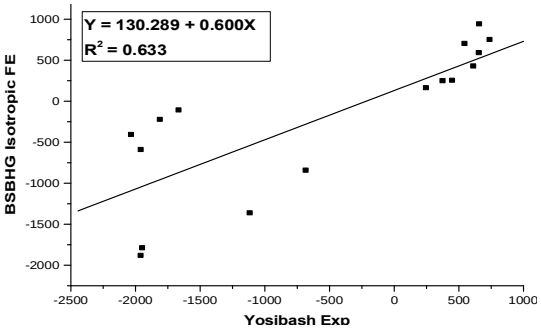


Fig. 12: Linear regression of predicted vs. experimental strain (με) in isotropic model

Low values of RMSE and maximum error are found for Wirtz/Peng, Wirtz/Peng-Krone and Rho-Peng Orthotropic models whereas isotropic model has recorded highest RMSE and analogously the maximum error.

In general, the regression strain results for isotropic model indicates that the overall behavior of isotropic BSBHG model is poor and this is due to higher difference in measured strain and predicted strain results at neck inferior location. Thus, the isotropic model is unable to capture structural heterogeneity in neck region.

Isotropic material model and Wirtz/Peng orthotropic material models have predicted reasonably same displacement results. But the same is not true for strain prediction results. The predicted strain results get improved with assignments of orthotropic results for Wirtz/Peng model. Hence the hypothesis presented by Peng et al.[19] and Baca et al. that "orthotropic material property assignment (global orthotropy) can be omitted, if the heterogeneous isotropic material model is used in FE analyses" is only true for displacement results but not for strain results.

| Validation on pooled data | $E$-$\mathcal{J}_{(app)}$ relationship implemented | | | | |
|---|---|---|---|---|---|
| | Isotropic model | Orthotropic material models | | | |
| | Wirtz | Taylor | Wirtz / Peng | Wirtz/Peng - Krone | Rho-Peng |
| $R^2$ | 0.633 | 0.923 | 0.951 | 0.959 | 0.945 |
| slope | 0.600 | 0.715 | 0.998 | 0.884 | 0.798 |
| Intercept(με) | 130.28 | 115.59 | 108.04 | 75.69 | 54.02 |
| RMSE( με) | 777.46 | 485.00 | 278.81 | 283.18 | 359.22 |
| RMSE % | 41.22 | 27.56 | 12.36 | 14.15 | 18.42 |
| max error ( με) | 1617 | 974 | 650 | 515 | 606 |
| Max error % | 85.74 | 55.34 | 28.81 | 25.72 | 31.08 |

Tab. 4: Evaluated validation parameter for different material models.

The results obtained in this investigation lead to conclusion that inclusion of material anisotropy improves the results over isotropic assumption.

Orthotropic bone model results are sensitive to material assignment relations and insensitive to orthotropic ratios. Further, it can also be concluded that material constants along with appropriate distribution of orthotropic ratios should be essential pre-requisites for any meaningful prediction of orthotropic FE analysis.

## 5 DISCUSSION

This study analyses the behavior of proximal femur for simple stance load condition using BSBHG FE model with varying degree of anisotropy in both cortical and cancellous bone. Four orthotropic material relations reported in literature have been considered for this purpose. Orthotropic ratio (i.e. $E_{33}$ / $E_{11}$ or $E_{33}$ / $E_{22}$) is location dependent. In present study, orthotropic model 1 (Taylor's model) shows same orthotropic ratio ($E_{33}$ / $E_{11}$= 1.71, $E_{33}$ / $E_{22}$ = 1.596) for both cancellous and cortical bone. This is due to the fact that a single relation has been used to define the properties of cortical and cancellous bone. In the other three orthotropic models (Peng model, Writz/Peng-Krone model, Rho-Peng model), orthotropic ratio is location dependent and density dependent. In these orthotropic models, two separate relations have been used to define cortical and cancellous bone.

It is interesting to note from the displacement results of orthotropic models that the results of Taylor's orthotropic model are in close agreement with experimental findings though orthotropic ratio is constant throughout bone for this model while displacement results of Peng's orthotropic model show good agreement with the isotropic model. The reason for this lies in the careful study of all orthotropic material models. From the study, it is revealed that Taylor's orthotropic model and Rho-Krone orthotropic model are able to predict meaningful elastic constants to model realistic stiffness of the real bone (see Fig. 2-4). It is also observed from the displacement results that Peng-Krone model is better than Peng's model though their Young's moduli are same for all values of apparent density. This may be due to the constant value of shear moduli ($G_{12}$, $G_{23}$, *and* $G_{13}$) assigned to regions of cancellous and cortical bone separately. As stated earlier, there is a small difference in isotropic-material-model and Peng orthotropic material model. Similar observation had been noted by Peng et al. [19], for two specific load conditions with similar material property assignment relation. They also concluded that either bone is weak orthotropic material or the load conditions used in his study were insensitive to orthotropic bone material character. But by observing other displacement results of our study one can conclude that bone orthotropy is sensitive to material assignment relation.

The regression results indicate that orthotropic material model predicts the strains with better accuracy than the isotropic model. A regression coefficient higher than 0.9 is obtained for all orthotropic models which is significantly higher than isotropic model regression coefficient $R^2$ = 0.63. The slope of regression line was not different from unity for Peng, Peng-Krone and isotropic model. But for Taylor's model and Rho-Peng model, slope of regression line is slightly higher than one, indicating that globally these two models underestimate the strains. As stated earlier, this may be due to the density-Young's modulus relationship we adopted.

Furthermore, the accuracy on the strains obtained with orthotropic models are considered to be in good agreement than the similar reported results (see Tab. 5) as in Keyak et al. [12], Ota et al. [18], Taddei et al. [27], Schielo et al. [26] and Helgason et al. [8].

| Strain validation | Model | $R^2$ | Slope |
|---|---|---|---|
| Keyak et al.[11] | voxel | 0.590 | 0.630 |
| Ota et al. [18] | Geometry based | 0.660 | Not Reported |
| Taddei et al. [27] | Geometry | 0.660-0.790 | 1.700-1.950 |

| | | | |
|---|---|---|---|
| | based | | |
| Schilo et al. [26] | Geometry based | 0.910 | 1.005 |
| Helgason et al. [8 ] | Geometry based | 0.790-0.850 | 1.700-1.500 |
| Present study | Geometry based | 0.920-0.960 | 0.710-0.998 |

Tab.5: Comparison of predicted strain results with published results.

Despite the advantages of our study, certain limitations also exist. First, in the present study, anisotropic evaluation analysis is carried out with BSBHG modeling methodology on a single specimen. Undoubtedly there is a need to carry out extensive study with meaningful model definition on a number of specimens. As stated in our previous study (Pise et al. [20]) some FE results are inconsistent at high degrees of freedom. This is due to low aspect ratio in some distorted elements in top slices of the proximal femur. It also shows low Jacobean value for these elements. This is unavoidable due to complex geometry of the specimen. However, despite this limitation, the importance and generality of the results obtained from this study is not reduced.

In summary, the global accuracy obtained with all orthotropic models is better than isotropic model presented in this paper. Further, it can also be concluded that material constants along with appropriate distribution of orthotropic ratios are essential pre-requisites for any meaningful prediction of orthotropic FE analysis.

## 6 CONCLUSION

A B-spline based heterogeneous modeling methodology is used to represent geometry and material estimation of both trabecular and cortical bone. In the current study FE model has been used with graded element approach to represent spatial distribution of material property in all direction which improves the performance of FE analysis. The results obtained in this investigation lead to conclusion that inclusions of material anisotropy improve the results over isotropic assumption. Also orthotropic bone model results are sensitive to material assignment relation rather than orthotropic ratios. Despite some limitation of the present model the orthotropic results are consistent and in better agreement for displacement with the reported experimental studies.

## 7 REFERENCES

[1] Bhatt, A. D.; Warkedkar, R.: Reverse engineering of human body: a B-spline based heterogeneous modeling approach, Computer- Aided Design and Application, 5, 2009, 194-208,doi:10.3722/cadaps.2008.

[2] Besso, M.; Ohnishi, I.; Matsuyams, J.; Matsumoto, T.; Imai, K.; Nkamura, K.: Predication of strength and strain of the proximal femur bt a ct based finite element method, Journal of Biomechanics, 40(8), 2007, 1745-1753,doi:10.1016/j.jbiomech.2006.08.003.

[3] Couteau, B.; Hobatho, M.C.; Darmana, R.; Brignola, J.C.; Arlaud, J. Y.: Finite element modeling of the vibrational behavior of the human femur using CT-based individualized geometrical and

material properties, Journal of Biomechanics, 31, 1998, 383ð386,doi:10.1016/S0021-9290(98)00018-9.

[4] Doblarè, M.; Garcia, J. M.: Anisotropic bone remodeling model based on a continuum damage repair theory, Journal of Biomechanics, 35, 2002, 1-17, doi:10.1016/S0021-9290(01)00178-6.

[5] Dong, X.N.; Guo, X.E.: The dependence of transverse isotropic elasticity of human femoral cortical bone on porosity, Journal of Biomechanics 37, 2004, 1281ð1,doi:10.1016/j.jbiomech.2003.12.011.

[6] Fung, Y.C.: A First course in Continuum Mechanics, Prentice hall, Inc Englewood Cliff NJ, 1968, 127-133.

[7] Gómez-Benito, M.J.; Garcia- Aznar, M. J.; Doblarè, M.: Finite element prediction of proximal femoral fracture patterns under different loads, Journal of Biomechanical Engineering, 127, 9-14, 2005, doi:10.1115/1.1835347.

[8] Halgason, B.; Taddei, F.; Palsson, H.; schilleo, E.; Cristofolini, L.; Viceconti, M.; Brynjolfsson, S.: A modified method for assigning material properties to FE model of bones, Medical Engineering and Physics, 30, 444-453, 2008, doi:10.1016/j.medengphy.2007.05.006.

[9] Jacobs, C. R.; Levenston, M. E.; Beaupre, G.S.; Simo, J. C.; Carter, D.R.: Numerical instabilities in bone remodeling simulation: The advantages of a node based finite element approach, Journal of Biomechanics, 28(4), 1995, 449ð459, doi: 10.1016/0021-9290(94)00087-K.

[10] Iyo, T.; Maki, Y.; Sasaki, N.; Nakata, M.: Anisotropic viscoelastic properties of cortical bone, Journal of Biomechanics, 37, 2004, 1433ð1437, doi:10.1016/j.jbiomech.2003.12.023.

[11] Keyak, J.H.; Meagher, J.M.; Skinner, H.B.; Mote, C.D.: Automated three-dimensional Finite element modeling of bone: a new method, Journal of Biomedical Engineering, 12(5), 1990, 389ð397, doi:10.1016/0141-5425(90)90022-F.

[12] Keyak, J.H.; Fourkas, M.G.; Meagher, J.M.; Skinner, H.B.: Validation of an automated method of three dimensional finite-element modeling bone, Journal of Biomedical Engineering, 15(6), 1993, 505ð9, doi:10.1016/0141-5425(93)90066-8.

[13] Kim, J. H.; Paulino, G. H.: Isoparametric graded finite elements for nonhomogeneous isotropic and orthotropic materials, ASME Journal of Applied Mechanics, 69, 2002, 502ð514, doi:10.11151/1.1467094.

[14] Krone,R.; Schuuter, P.: An investigation on the importance of material anisotropy in finite-element modeling of human femur, 2006 SAE international, Paper no 2006-01-0064.

[15] Lotz, J. C.; Gerhart, T. N.; Hayes, W. C.: 1991a, Mechanical Properties of Metaphyseal Bone in the Proximal Femur, J. Biomech., 24, 1991, 317ð329, doi:10.101610021-9290(91)90350-V.

[16] Lotz, J. C.; Cheal, E. J.; Hayes, W. C.: 1991b, Fracture Prediction for the Proximal Femur Using Finite Element Models: Part 1 ñ Linear Analysis, J. Biomech. Eng., 113, 1991, 353ð360.

[17] Merz, B.; Niederer, P.; Muller, R.; Ruegsegger, P.: Automated finite element analysis of excised human femora based on precision QCT, Journal of Biomechanical Engineering, 118(3), 1996, 387-390.

[18] Ota, T.; Yamamoto, I.; Morita, R.: Fracture simulation of the femoral bone using the finite element method: how a fracture initiates and proceeds, Journal of bone and mineral metabolism, 17, 1999, 108-112.

[19] Peng, L.; Bai, J.; Zeng, X.; Zhou Y.: Comparison of isotropic and orthotropic material property assignments on femoral finite element models under two loading conditions, Medical Engineering and Physics, 18, 2006, 227 -233.

[20] Pise, U.V.; Bhatt, A.D.; Srivastava, R. K.; Warkedkar, R.: A B-spline based heterogeneous modeling and analysis with graded element, Journal of Biomechanics, 2009, doi:10.1016/j.jbiomech.2009.05.019

[21] Qian, X.; Dutta, D.: Feature based design for heterogeneous objects, Computer-Aided Design, 36(12), 2004, 1263ð78, doi:10.1016/j.cad.2004.01.012.
[22] Reilly, D.T.; Burstein, A.H.: The elastic and ultimate properties of compact bone tissue, Journal of Biomechanics, 8, 1975, 393ð405,doi:10.1016/0021-9290(75)90075-5.
[23] Rho, J.Y.; Hobatho, M.C.; Ashman, R.B.; Relations of mechanical properties to density and CT numbers in human bone, Medical Engineering and Physics, 17(5), 1995, 347ð55, doi:10.1016/1350-4533(95)97314-F.
[24] Rohlmann, A.; Mössner, U.; Bergmann, G.; Kölbel, R.: Finite ðelement-analysis and experimental investigation of stresses in a femur, Journal of Biomedical Eng. 4, 1982, 241-246, doi:10.1016/0141-5425(82)90009-7.
[25] Santare, M. H.; Lambros, J.: Use of graded finite elements to model the behavior of nonhomogeneous materials, ASME Journal of Applied Mechanics, 67, 2000, 819ð822.
[26] Schilleo, E.; Taddei, F.; Malandrao, A.; Cristofolini, L.; Viceconti, M.: Subject-specific finite element models can accurately predict strain levels in long bones, Journal of Biomechanics, 40, 2007, 2928-2989, doi:10.1016/j.jbiomech2007.02.010.
[27] Shahar, R.; Zalansky, P.; Brak, M.; Friessem, A.; Currey, J.; Weiner, S.: Anisotropic Poissonîs ratio and compression modulus of cortical bone determined by speckle interferometry, Journal of Biomechanics 40, 2007, 252-264,doi:10.1016/j.jbiomech.2006.01.021.
[28] Stɔlpner, M. A.; Reddy, B. D.; Starke, G. R.; Spirakis, A.: A three dimensional finite analysis of adaptive remodeling in the proximal femur, Journal of Biomechanics, 30, 1997, 1063ð1067, doi:10.1016/S0021-9290(97)000742.
[29] Taddei, F.; Pancanti, A.; Viceconti, M.: An improved method for the automatic mapping of computed tomography numbers onto finite element models, Medical Engineering and Physics, 26 (1), 2004, 61ð69,doi:10.1016/S1350-4533(03)00138-3.
[30] Taddei, F.; Schilo, E.; Hegason, B.; Cristofolini, L.; Viceconti, M.: The material mapping strategy influences the accuracy of CT-based finite element models of bines: an evaluation against experimental measurements, Medical Engineering and Physics, 29, 2007, 973-979,doi:10.1016/j.medengphy.2006.10.014.
[31] Taylor, W.R.; Roland, E.; Ploeg, H.; Hertig, D.; Klabunde, R.; Warner, M.D.; Hobatho, M. C.; Rakotomanana, L.; Clift, S. E.: Determination of orthotropic bone elastic constants using FEA and Modal analysis, Journal of Biomechanics, 35, 2002, 767ð773, doi:10.1016/S0021-9290(02)00022-2.
[32] Verhulp, E.; Rietbergen, B. V.; Huiskes, R.: Comparison of micro-level and continuum-level voxel models of the proximal femur, Journal of Biomechanics 39(4), 2006, 2951ð2957,doi:10.1016/j.jbiomech.2005.10.027.
[33] Warkhedkar, R.M.; Bhatt, A.D.: Material-solid modeling of human body: A heterogeneous B-spline based approach, Computer-Aided Design, 2008, doi:10.1016/j.cad.2008.10.016.
[34] Wirtz, D.C.; Schiffers, N.; Pandorf, T.; Radermacher, K.; Weichert, D.; Forst, R.: Critical evaluation of known bone material properties to realize anisotropic FE- simulation of the proximal femur, Journal Biomechanical Engineering, 33, 2000, 1325-1330, doi:10.1016/S0021-9290(00)00069-5
[35] Wirtz, D.C.; Pandorf, T.; Portheine, F.; Radermache, K.; Schiffers, N.; Prescher, A.; Weichert, D.; Ncthard, F.U.: Concept and development of an orthotropic FE model of the proximal femur, Journal of Biomechanics, 36, 2003, 289ð293, doi:10.1016/S0021-9290(02)00309-3.
[36] Yang, P.; Qian, X.: A B-spline-based approach to heterogeneous objects design and analysis, Computer-Aided Design, 39, 2007, 95ð111, doi:10.1016/j.cad.2006.10.005.

[37] Yosibash, Z.; Padan, R.; Joskowicz, L.; Milgrom, C.: A CT-based high-order finite element analysis of the human proximal femur compared to in- vitro experiments, Journal of Biomechanical Engineering 129, 2007, 297-309.

[38] Zannoni, C.; Mantovani, R.; Viceconti, M.: Material properties assignment to finite element models of bone structures: a new method, Medical Engineering and Physics 20 (10), 735ð740, 1998, doi:10.1016/S1350-4533(98)00081-2.